 CMES, vol.3, no.4, pp.455-464, 2002

Thermohydrodynamic Analysis of Journal Bearings Lubricated with Multigrade Oils

J.Y. Jang[1] **and M.M. Khonsari**[2]

Abstract: Thermohydrodynamic analysis of journal bearings lubricated with multigrade oils is presented. Design charts are presented that enable one to readily estimate the bearing maximum temperature and the shaft temperature using a series of dimensionless parameters introduced in this paper.

Nomenclature

C	Clearance (m)
c_o	Lubricant specific heat $(J/Kg\ K)$
D	Diameter of the shaft (m)
h	Film thickness (m)
h_{conv}	Convective heat transfer coefficient (W/m^2K)
k_b	Thermal conductivity of the bushing (W/mK)
k_o	Thermal conductivity of the lubricant (W/mK)
L	Bearing length in the axial direction (m)
N	Shaft speed (rpm)
P	Pressure (Pa)
P_a	Ambient pressure (Pa)
$P_{\max}$	Maximum pressure (Pa)
P_s	Supply pressure (Pa)
Q_{rec}	Recirculating flow rate (m^3/s)
Q_s	Supply flow rate (m^3/s)
R	Radius of the shaft (m)
R_{bi}	Inner radius of the bushing (m)
R_{bo}	Outer radius of the shaft (m)
T	Temperature $(^\circ\text{C})$
T_a	Ambient temperature $(^\circ\text{C})$
T_b	Temperature of the bushing $(^\circ\text{C})$
$T_{\max}$	Maximum temperature $(^\circ\text{C})$
T_{mix}	Mixing temperature $(^\circ\text{C})$
T_{rec}	Recirculating temperature $(^\circ\text{C})$
T_{shaft}	Shaft temperature $(^\circ\text{C})$
T_s	Lubricant temperature supplied $(^\circ\text{C})$
U	Velocity of the shaft (m/s)
u, v, w	Velocity component along, across the film and in the axial direction (m/s)
W	Bearing load-carrying capacity (N)
x, y, z	Coordinate system (m)
r_b, θ_b	Coordinate system used in the bushing (m)
β	Zero-shear-rate viscosity vs. temperature coefficient $(1/K)$
β_∞	Infinite-shear-rate viscosity vs. temperature coefficient $(1/K)$
β_σ	Curve fitting variable vs. temperature coefficient $(1/K)$
ε	Eccentricity ratio
$\dot{\gamma}$	Shear rate $(1/s)$
η	Non-Newtonian viscosity $(Pa \cdot s)$
κ_1, κ_2	Temperature-rise parameters
μ_0	Zero-shear-rate viscosity $(Pa \cdot s)$
μ_{0i}	Initial zero-shear-rate viscosity $(Pa \cdot s)$
μ_∞	Infinite-shear-rate viscosity $(Pa \cdot s)$
ρ_o	Density of the lubricant (Kg/m^3)
σ	Curve fitting variable (Pa)
τ	Shear stress (Pa)
ω	Angular velocity of the shaft (rad/s)
Λ	Aspect ratio of the journal bearing

[1] Center for Advanced Friction Studies
Southern Illinois University
Carbondale, IL 62901-4343
[2] Corresponding Author
Department of Mechanical Engineering
Louisiana State University
Baton Rouge, LA 70803

1 Introduction

The classical hydrodynamic lubrication theory assumes that the lubricant behaves essentially as a linearly viscous (Newtonian) fluid. There exists, however, an important class of lubricants that can not be classified as Newtonian. Analytical and computational tools are needed

to accurately predict performance of bearings lubricated with such lubricants. Various modeling schemes are available for this purpose. Of particular interest is a class of non-Newtonian lubricants in which the apparent viscosity decreases with increasing rate of shear if the temperature and mean temperature remain constant. This type of lubricants is classified as a shear-thinning fluid and there are several rheological expressions available for expressing their behavior. Tanner (1963) applied the power law model as a constitutive equation to model an infinitely short journal bearing. Dien and Elrod (1983) also used the power model to solve the Couette-dominated flow in the infinitely wide slider bearing and journal bearing. Buckholz (1986) followed the same procedure as Dien and Elrod for the Couette-dominated flows in plane slider bearing, and compared to the matched asymptotic theory.

The power law model is a very simple and widely used constitutive equation. However, Gecim (1990) showed that the power law model fails to match the viscosity of multigrade oils - that are commonly used for the engine lubrication - at the low or high ends of the shear rate spectrum. Using a general apparent-viscosity function for the constitutive equation taking into account most of the rheological laws, Gecim derived a governing differential equation, similar to the generalized Reynolds equation reported by Dowson (1962) for Newtonian fluids. Another noteworthy contribution is the work of Wada and Hayashi (1971a,b) who formulated a polynomial constitutive equation for a commercial base oil and several derivatives of it containing controlled amount of polymer additions.

This paper is devoted to the study of journal bearings lubricated with multigrade oils. For this purpose, a comprehensive thermohydrodynamic analysis (THD) is developed and the results of extensive amount of simulations are presented in the form of design charts.

2 Governing Equations

2.1 Constitutive Equation

Experimental data for shear stress τ versus shear rate $\dot{\gamma}$ of shear thinning fluids or shear thickening fluids, presented in a log-log coordinate system, shows that a straight line is very often observed in over two or three logarithmic decades of shear rate $\dot{\gamma}$. Therefore, the simplest fluid model to express the shear thinning fluids is the power law model of Ostwald-de Waele. That is:

$$\tau = m\dot{\gamma}^n \tag{1}$$

where m and n are the rheological parameters of the model, and the constitutive relation becomes $\eta = m\dot{\gamma}^{n-1}$. For n=1 equation (1) describes the Newtonian fluids. For n¡1 it describes the shear thinning fluids. For n¿1 it describes the shear thickening fluids.

For shear thinning fluids, the power law model predicts $\eta \to \infty$ for $\dot{\gamma} \to 0$ and $\eta \to 0$ for $\dot{\gamma} \to \infty$. In reality, in both cases of shear rate approaching zero and approaching infinity, the value of viscosity η approaches a constant finite value. These values are the zero-shear-rate viscosity μ_0 and the infinite-shear-rate viscosity μ_∞, respectively. In the case of n¡1, one has $\mu_0 > \mu_\infty$. Therefore, a non-Newtonian shear thinning fluid has three distinct regions (cf. Ferguson and Kemblowski, 1991):

- The Newtonian region at low shear rates $\dot{\gamma}$ which is referred to as the lower Newtonian region. The flow is characterized by a constant zero-shear-rate viscosity μ_0.
- Non-Newtonian region of intermediate shear rate. The flow is characterized by a shear dependent viscosity η.
- The Newtonian region at high shear rates $\dot{\gamma}$ which is referred to as the upper Newtonian region. The flow is characterized by a constant infinite-shear-rate viscosity μ_∞.

Gecim (1990) proposed a new model for shear thinning fluids expressed as:

$$\eta_j = \mu_0 \frac{\sigma + \mu_\infty \left|\dot{\gamma}_j\right|}{\sigma + \mu_0 \left|\dot{\gamma}_j\right|}, \qquad j = x, z \tag{2}$$

where $\dot{\gamma}_x = \frac{\partial u}{\partial y}$ and $\dot{\gamma}_z = \frac{\partial w}{\partial y}$. Parameter σ is a curve fitting variable representing the shear stability of the lubricant. From Figure 1, high value of σ indicates greater shear stability. At low shear rates, σ is much greater than other terms. Hence, the viscosity approaches the zero-shear-rate viscosity μ_0. At high shear rates, σ is much smaller than other terms, and the viscosity approaches the infinite-shear-rate viscosity μ_∞. The curve fitting parameter σ determines the range of shear rate where diversion between zero-shear-rate viscosity μ_0 and infinite-

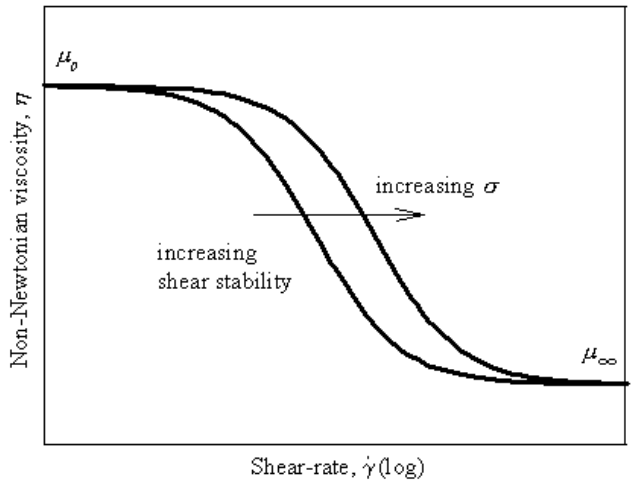

Figure 1 : Variation of non-Newtonian viscosity

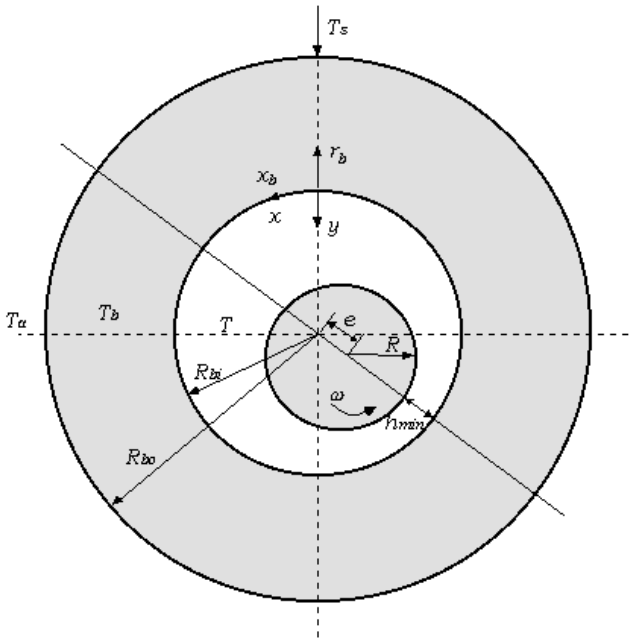

Figure 2 : Cross-section of the journal bearing

shear-rate viscosity μ_∞ takes place. Therefore, the constitutive equation proposed by Gecim describes three regions of shear thinning fluids described above. It is important to note that this constitutive equation (2) treats the viscosity as a vector and is dependent upon the coordinate system. Paranjpe (1992) has modified the constitutive equation proposed by Gecim in the following form:

$$\eta = \mu_0 \frac{\sigma + \mu_\infty \dot{\gamma}}{\sigma + \mu_0 \dot{\gamma}} \tag{3}$$

This model describes shear thinning fluids, such as multigrade engine oils, particularly well. We shall make use of this constitutive equation in treating multigrade oils.

Using $\overline{\mu}_0 = \frac{\mu_0}{\mu_{0i}}$, $\overline{\mu}_\infty = \frac{\mu_\infty}{\mu_{0i}}$ and $\overline{\sigma} = \frac{C\sigma}{\mu_{0i}U}$, the dimensionless non-Newtonian viscosity becomes:

$$\overline{\eta} = \overline{\mu}_0 \frac{\overline{h}\overline{\sigma} + \overline{\mu}_\infty \dot{\overline{\gamma}}}{\overline{h}\overline{\sigma} + \overline{\mu}_0 \dot{\overline{\gamma}}} \tag{4}$$

2.2 Generalized Reynolds Equation

A cross-section of a journal bearing showing the nomenclature of the problem is presented in Figure 2. By replacing the non-Newtonian viscosity $\overline{\eta}$ instead of Newtonian viscosity $\overline{\mu}$ the governing equations for Newtonian fluids are equally valid for a simple non-Newtonian fluids. Therefore, the dimensionless form of the generalized Reynolds equation for the shear thinning fluids becomes:

$$\frac{\partial}{\partial \overline{x}}\left[\overline{h}^3\left(\frac{\partial \overline{P}}{\partial \overline{x}}\right)\overline{F}_2\right] + \frac{1}{4\Lambda^2}\frac{\partial}{\partial \overline{z}}\left[\overline{h}^3\left(\frac{\partial \overline{P}}{\partial \overline{z}}\right)\overline{F}_2\right] = \frac{d\overline{h}}{d\overline{x}} - \frac{\partial}{\partial \overline{x}}\left(\frac{\overline{F}_1}{\overline{F}_0}\right) \tag{5}$$

where

$$\begin{aligned}
&\overline{x} = \frac{x}{R}, \quad \overline{y} = \frac{y}{h}, \qquad \overline{z} = \frac{z}{L}.\\
&\overline{h} = \frac{h}{C}, \quad \overline{P} = \frac{C^2 P}{\mu_{0i} R U}, \quad \Lambda = \frac{L}{D},\\
&\overline{F}_0 = \int_0^1 \frac{1}{\overline{\eta}} d\overline{y}, \quad \overline{F}_1 = \int_0^1 \frac{\overline{y}}{\overline{\eta}} d\overline{y},\\
&\overline{F}_2 = \int_0^1 \frac{\overline{y}}{\overline{\eta}}\left(\overline{y} - \frac{\overline{F}_1}{\overline{F}_0}\right) d\overline{y}
\end{aligned} \tag{6}$$

The boundary conditions are:

$$\begin{aligned}
&\overline{P} = \overline{P}_s \text{ at } \overline{x} = \overline{x}_{\text{inlet}} = 0,\\
&\overline{P} = \overline{P}_a = 0 \text{ at } \overline{z} = \pm\frac{1}{2},\\
&\frac{\partial \overline{P}}{\partial \overline{x}} = 0 \text{ and } \overline{P} = \overline{P}_a = 0 \text{ at } \overline{x} = \overline{x}_{\text{cav}}
\end{aligned} \tag{7}$$

The first boundary condition pertains to an axial groove located at the top of the journal bearing. The third boundary condition represents the Swift-Stieber boundary condition.

2.3 Energy Equation

It has been shown that a two-dimensional energy equation, assuming that temperature remains uniform in the axial direction, can be used for a successful thermohydrodynamic model of journal bearings. This simplifying assumption results in a realistic prediction of the bearing performance with a considerable amount of savings in computational time (Khonsari and Beaman, 1986). Thus, the energy equation in dimensionless form for the incompressible, laminar flow can be written as:

$$\begin{aligned}
&\overline{u}\frac{\partial\overline{T}}{\partial\overline{x}}+\frac{1}{\overline{h}}\left(\overline{v}-\overline{uy}\frac{d\overline{h}}{d\overline{x}}\right)\frac{\partial\overline{T}}{\partial\overline{y}}\\
&\quad+\frac{1}{\lambda_1}\left[-2\frac{\overline{y}}{\overline{h}^2}\left(\frac{d\overline{h}}{d\overline{x}}\right)^2+\frac{\overline{y}}{\overline{h}}\left(\frac{d^2\overline{h}}{d\overline{x}^2}\right)\right]\frac{\partial\overline{T}}{\partial\overline{y}}\\
&\quad=\frac{1}{\lambda_1}\frac{\partial^2\overline{T}}{\partial\overline{x}^2}+\frac{\lambda_2}{\lambda_1}\frac{1}{\overline{h}^2}\frac{\partial^2\overline{T}}{\partial\overline{y}^2}+\frac{1}{\lambda_1}\frac{\overline{y}}{\overline{h}^2}\left(\frac{d\overline{h}}{d\overline{x}}\right)^2\frac{\partial^2\overline{T}}{\partial\overline{y}^2}\\
&\quad-2\frac{1}{\lambda_1}\frac{\overline{y}}{\overline{h}}\left(\frac{d\overline{h}}{d\overline{x}}\right)\frac{\partial^2\overline{T}}{\partial\overline{x}\partial\overline{y}}+\frac{\lambda_3}{\lambda_1}\frac{1}{\overline{h}^2}\overline{\eta}\left(\dot{\overline{\gamma}}\right)\left[\left(\frac{\partial\overline{u}}{\partial\overline{y}}\right)^2+\left(\frac{\partial\overline{w}}{\partial\overline{y}}\right)^2\right]
\end{aligned}\tag{8}$$

where $\overline{T}=\beta(T-T_s)$, $\lambda_1=\frac{\rho_o c_o UR}{k_o}$, $\lambda_2=\left(\frac{R}{C}\right)^2$ and $\lambda_3=\left(\frac{R}{C}\right)^2\frac{\mu_{0i}\beta U^2}{k_o}$. The parameter β is the zero-shear-rate viscosity vs. temperature coefficient.

The boundary conditions for THD solution at the oil-shaft interface and the oil-bush interface are (Khonsari and Beaman, 1986):

$$\begin{aligned}
&\int_0^{2\pi}\left.\frac{\partial\overline{T}}{\partial\overline{y}}\right|_{\overline{y}=1}d\overline{x}=0 \text{ and } \left.\overline{T}\right|_{\overline{y}=1}=\overline{T}_{\text{shaft}}\\
&\left.\frac{\partial\overline{T}}{\partial\overline{y}}\right|_{\overline{y}=0}=-\overline{h}\frac{Ck_b}{R_{bi}k_o}\left.\frac{\partial\overline{T}_b}{\partial\overline{r}_b}\right|_{\overline{r}_b=\overline{R}_{bi}}
\end{aligned}\tag{9}$$

If an adiabatic condition is imposed at the inner surface of the bush, boundary conditions simplify to:

$$\begin{aligned}
&\int_0^{2\pi}\left.\frac{\partial\overline{T}}{\partial\overline{y}}\right|_{\overline{y}=1}d\overline{x}=0 \text{ and } \left.\overline{T}\right|_{\overline{y}=1}=\overline{T}_{\text{shaft}}\\
&\left.\frac{\partial\overline{T}}{\partial\overline{y}}\right|_{\overline{y}=0}=0
\end{aligned}\tag{10}$$

Boundary conditions given in equation (**??**) are referred as ISOADI (the isothermal condition at the oil-shaft interface and the adiabatic condition at the oil-bush interface). Even though the ISOADI solutions result in somewhat higher temperatures than those measured experimentally, they are realistic and provide conservative estimates of $T_{\max}$, pressure profile and bearing performance.

The temperature of the recirculating fluid is normally higher than the temperature of the incoming supply lubricant T_s. Thus, the recirculating flow transfers a portion of its thermal energy to the supply oil at the inlet. An energy balance at the inlet gives (Khonsari et al., 1996):

$$\overline{T}_{\text{mix}}=\frac{\overline{T}_{\text{rec}}\overline{Q}_{\text{rec}}}{\overline{Q}_{\text{rec}}+\overline{Q}_s}\tag{11}$$

where $\overline{Q}_s$ is the supplied flow rate which is the same amount as the leakage rate. Due to cavitation in the divergent section of the bearing, the film is incomplete and the bearing is only partially covered with lubricant over the length (Khonsari & Booser, 2001). Thus, it is necessary to account for the thermal characteristics of the lubricant in the cavitation zone. The thermal characteristics are corrected in the cavitation zone by using the effective length of fluid film. This correction is thought to be realistic for assessment of cavitation effects in a steadily loaded journal bearing. On the other hand, for a dynamically loaded journal bearing, it may be necessary to implement a mass conservative boundary condition. The interested reader is referred to the work of Paranjpe (1992) on this subject.

Physically, the fluid heat conduction term in the circumferential direction is very small when compared with other terms (Dowson et. al., 1966). Neglecting small terms with $1/\lambda_1$ multiplier, the dimensionless energy equation becomes:

$$\begin{aligned}
&\overline{u}\frac{\partial\overline{T}}{\partial\overline{x}}+\frac{1}{\overline{h}}\left(\overline{v}-\overline{uy}\frac{d\overline{h}}{d\overline{x}}\right)\frac{\partial\overline{T}}{\partial\overline{y}}\\
&\quad=\frac{\kappa_1}{\kappa_2^2}\frac{1}{\overline{h}^2}\frac{\partial^2\overline{T}}{\partial\overline{y}^2}+\kappa_1\frac{1}{\overline{h}^2}\overline{\eta}\left(\dot{\overline{\gamma}}\right)\left[\left(\frac{\partial\overline{u}}{\partial\overline{y}}\right)^2+\left(\frac{\partial\overline{w}}{\partial\overline{y}}\right)^2\right]
\end{aligned}\tag{12}$$

where two key parameters appear in the dimensionless energy equation. They are defined as follows:

$$\begin{aligned}
&\kappa_1\equiv\frac{\lambda_3}{\lambda_1}=\frac{\alpha_o}{k_o}\mu_{0i}\beta\omega\left(\frac{R}{C}\right)^2\\
&\kappa_2\equiv\sqrt{\frac{\lambda_3}{\lambda_2}}=\sqrt{\frac{\mu_{0i}\beta}{k_o}}U
\end{aligned}\tag{13}$$

The first temperature-rise parameter, κ_1, is associated with the viscous dissipation. It incorporates all of the oil properties, shaft velocity and bearing geometry. The second temperature-rise parameter, κ_2, incorporates the oil properties and the linear velocity. These temperature-rise parameters describe the temperature field in the fluid film.

The zero-shear-rate viscosity decreases exponentially with increasing temperature according to:

$$\overline{\mu}_0 = e^{-\overline{T}} \tag{14}$$

In addition to the temperature-rise parameters κ_1 and κ_2, two additional independent parameters $\overline{\sigma}$ and $\overline{\mu}_\infty$ appear in the non-Newtonian viscosity associated with the dimensionless energy equation for the multigrade engine oil. These four parameters directly influence the temperature field of the multigrade oil. Generally the curve fitting variable, $\overline{\sigma}$, increases with increasing temperature as prescribed by the following relationship:

$$\overline{\sigma} = \overline{\sigma}_i e^{\overline{\beta}_\sigma \overline{T}} \tag{15}$$

where dimensionless curve fitting variable vs. temperature coefficient $\overline{\beta}_\sigma = \beta_\sigma/\beta$. In present analysis $\overline{\beta}_\sigma$ is assumed to be unity, which implies $\beta_\sigma = \beta$. On the other hand, the infinite-shear-rate viscosity, $\overline{\mu}_\infty$, tends to decrease with increasing temperature and defined according to:

$$\overline{\mu}_\infty = \overline{\mu}_{\infty_i} e^{-\overline{\beta}_\infty \overline{T}} \tag{16}$$

where $\overline{\beta}_\infty = \beta_\infty/\beta$. The ratio of infinite-shear-rate viscosity to zero-shear-rate viscosity, μ_∞/μ_0, is always a constant independent of the temperature variation (cf. Wright et al., 1983). This implies that $\beta_\infty = \beta$ $(\overline{\beta}_\infty = 1)$.

2.4 Heat Conduction Equation

The heat conduction equation in the bushing is coupled with the energy equation by these boundary conditions. The dimensionless heat conduction equation is:

$$\frac{\partial^2 \overline{T}_b}{\partial \overline{r}_b^2} + \frac{1}{\overline{r}_b}\frac{\partial \overline{T}_b}{\partial \overline{r}_b} + \frac{1}{\overline{r}_b^2}\frac{\partial^2 \overline{T}_b}{\partial \overline{\theta}_b^2} = 0 \tag{17}$$

On the outer surface of the bushing, heat loss takes place by convection to the ambient, i.e.,

$$\left.\frac{\partial \overline{T}_b}{\partial \overline{r}_b}\right|_{\overline{r}_b=\overline{R}_{bo}} = -\frac{h_{conv}}{k_b} R_{bi}\left(\left.\overline{T}_b\right|_{\overline{r}_b=\overline{R}_{bo}} - \overline{T}_a\right) \tag{18}$$

3 Results

The governing equations and the boundary conditions presented in section 2 were solved using the finite difference method. The details of solution schemes are given by Khonsari et al. (1996).

3.1 Validation

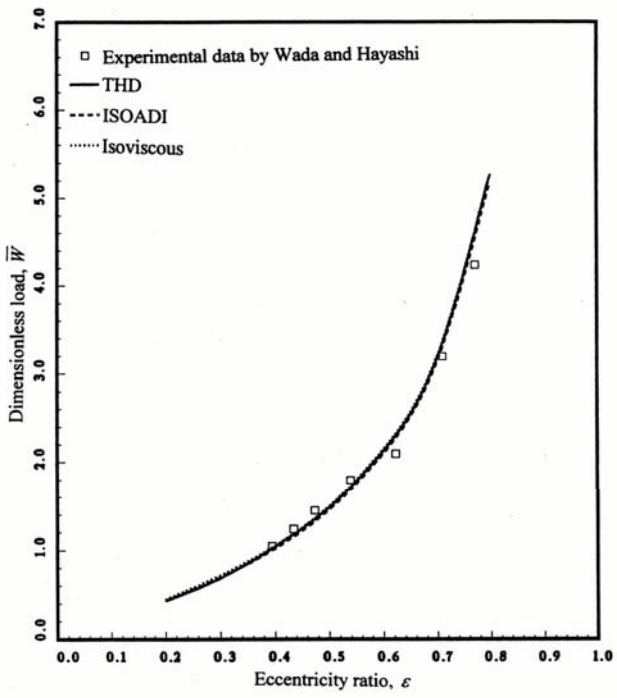

Figure 3 : Comparison of load capacity with the experiments by Wada and Hayashi ($\Lambda = 1; N = 308$ rpm)

Published experimental results with multigrade oils are rare. However, a limited set of experimental results due to Wada and Hayashi (1971b) is available. Figure 3 presents the variation of dimensionless load capacity as a function of the eccentricity ratio based on the THD, ISOADI and isoviscous analyses. The lubricant is a spindle oil to which 0.3% polyisobutylene is added. The results of the present theories are compared to the experimental measurements by Wada and Hayashi. The present results are in good agreement with the experimental measurements. The solutions of THD, ISOADI, and isoviscous analyses are very close since the rotational speed N=308 *rpm* is very small leading to the insignificant temperature rise. Figure 4 shows the pressure distribution based on THD, ISOADI, and isoviscous analyses. The

present pressure distributions are in good agreement with the experimental pressure measurements.

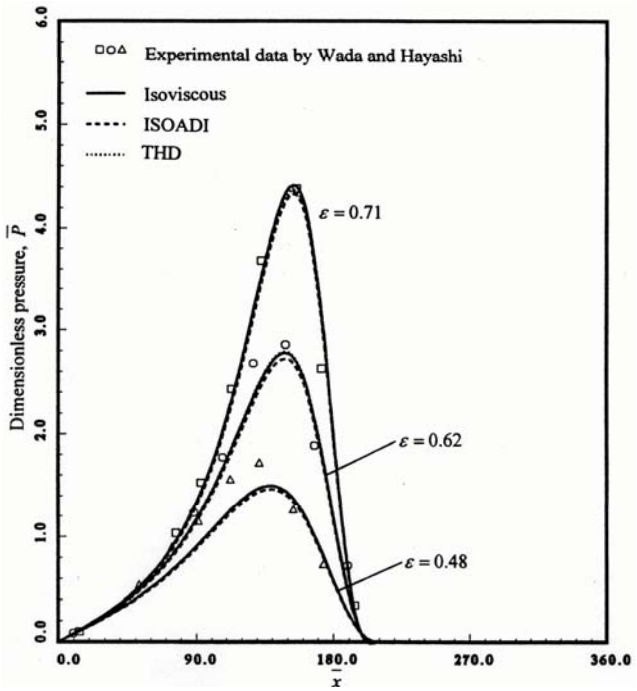

Figure 4 : Comparison of presure distribution with the experiments by Wada and Hayashi ($\Lambda = 1; N = 308$ rpm)

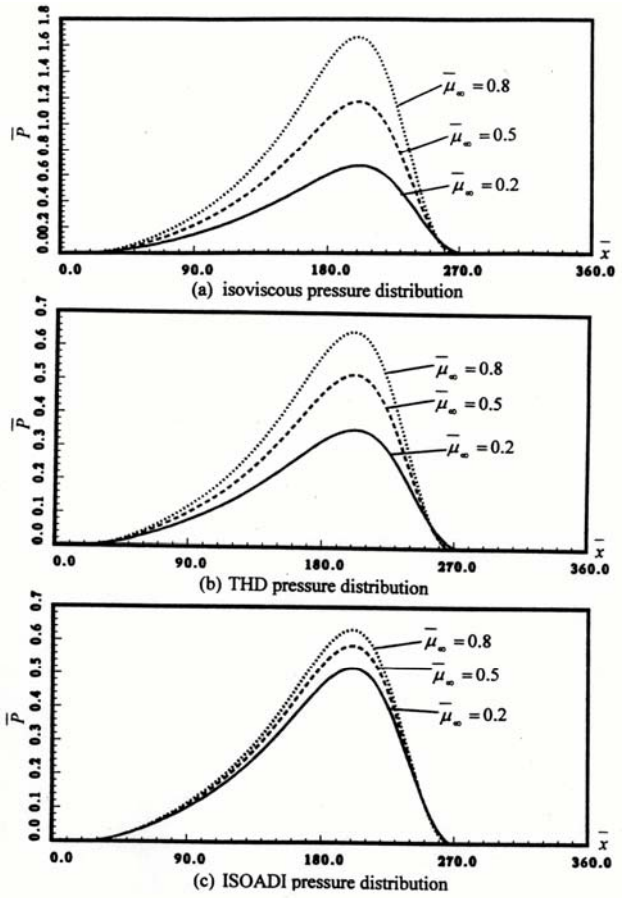

Figure 5 : Isoviscous, THD and ISOADI pressure distributions of a journal bearing ($\varepsilon = 0.5; \Lambda = 1; \kappa_1 = 0.15; \kappa_2 = 1.5$)

3.2 Parametric Study

Figure 5 shows the typical case of the isoviscous, THD and ISOADI pressure distribution of a finite journal bearing at ε=0.5. The temperature rise parameters κ_1=0.15 and κ_2=1.5 are used for the THD and ISOADI analyses. The maximum pressure occurs around 210°. The maximum pressure increases with increasing $\overline{\mu}_\infty$ since the non-Newtonian viscosity $\overline{\eta}$ becomes greater. The isoviscous maximum pressure is much higher than the THD and ISOADI maximum pressure since the viscosity evaluated at the supply temperature is used for the isoviscous analysis. At a relatively low $\overline{\mu}_\infty$, the ISOADI maximum pressure is higher than the THD maximum pressure since $\overline{\sigma}$ is a dominant parameter. Also, the ISOADI non-Newtonian viscosity is more stable due to the higher temperature. At $\overline{\mu}_\infty$=0.8, the THD maximum pressure is somewhat higher than the ISOADI maximum pressure since the effect of $\overline{\sigma}$ is reduced and the behavior of the fluid becomes much like a linear viscous (Newtonian) fluid. Figure 6 and 7 shows the THD and ISOADI isotherm contours of the lubricant, respectively. Similar to Newtonian fluids, the maximum temperature predicted for multigrade oil occurs near the minimum film thickness. At a relatively high $\overline{\mu}_\infty$, the maximum and shaft temperatures are higher than those at a lower $\overline{\mu}_\infty$ since $\overline{\eta}$ becomes greater and more frictional heat generated. ISOADI temperature distribution is relatively higher than THD temperature distribution as expected.

Figure 8 shows how $\overline{T}_{\max}$ and $\overline{T}_{\text{shaft}}$ vary with dimensionless infinite-shear-rate viscosity, $\overline{\mu}_\infty$, according to the ISOADI predictions. These simulations correspond to the temperature-rise parameters κ_1=0.15 and κ_2=1.5. Both $\overline{T}_{\max}$ and $\overline{T}_{\text{shaft}}$ tend to increase with increasing $\overline{\mu}_\infty$ and $\overline{\sigma}$. At a relatively low $\overline{\mu}_\infty$, both $\overline{T}_{\max}$ and $\overline{T}_{\text{shaft}}$ increase rapidly since the variation of the non-Newtonian viscosity is sensitive. For $\overline{\mu}_\infty$=1 the fluid behaves as a Newtonian and, therefore, $\overline{T}_{\max}$ and $\overline{T}_{\text{shaft}}$ become independent of $\overline{\sigma}$.

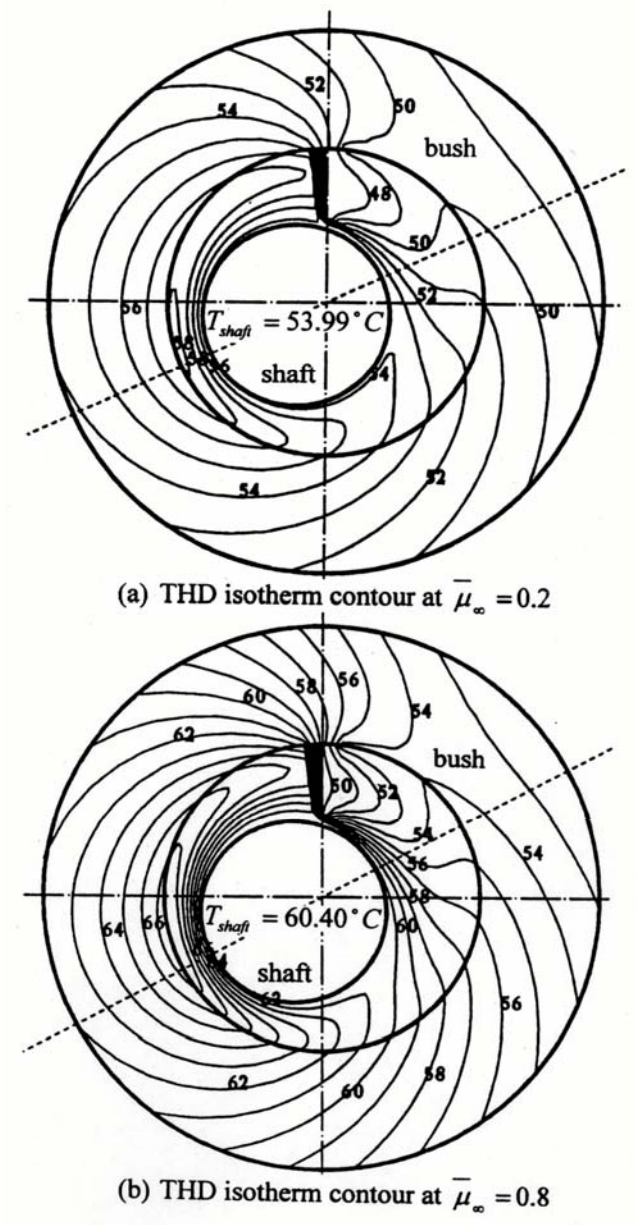

Figure 6 : THD isotherm contour in the lubricant at *overline*$\mu_{\infty} = 0.2$ and *overline*$\mu_{\infty} = 0.8$ ($T_s = 40^{\circ}$C; $\varepsilon = 0.5$; $\Lambda = 1$; $\kappa_1 = 0.15$; $\kappa_2 = 1.5$)

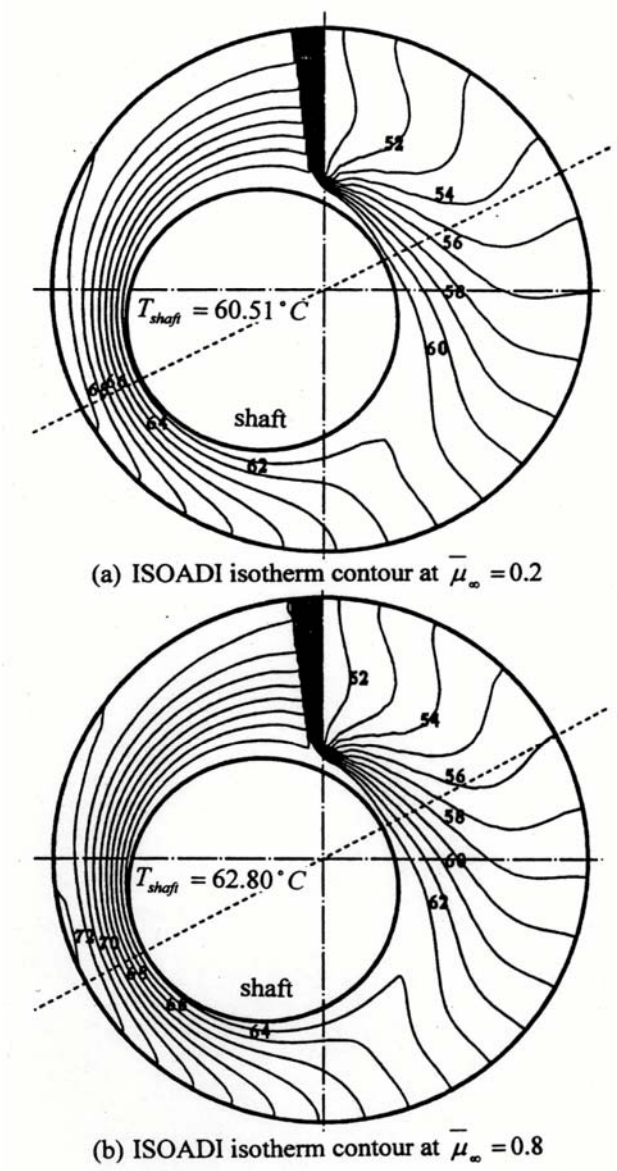

Figure 7 : ISOADI isotherm contour in the lubricant at *overline*$\mu_{\infty} = 0.2$ and *overline*$\mu_{\infty} = 0.8$ ($T_s = 40^{\circ}$C; $\varepsilon = 0.5$; $\Lambda = 1$; $\kappa_1 = 0.15$; $\kappa_2 = 1.5$)

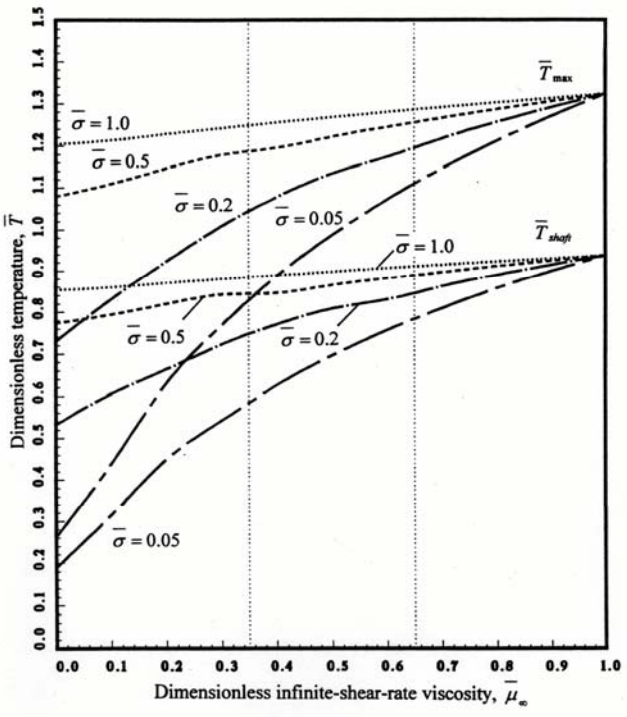

Figure 8 : Effect of infinite-shear-rate viscosity on the maximum temperature and shaft temperature of a journal bearing ($\varepsilon = 0.5$; $\Lambda = 1$; $\kappa_1 = 0.15$; $\kappa_2 = 1.5$)

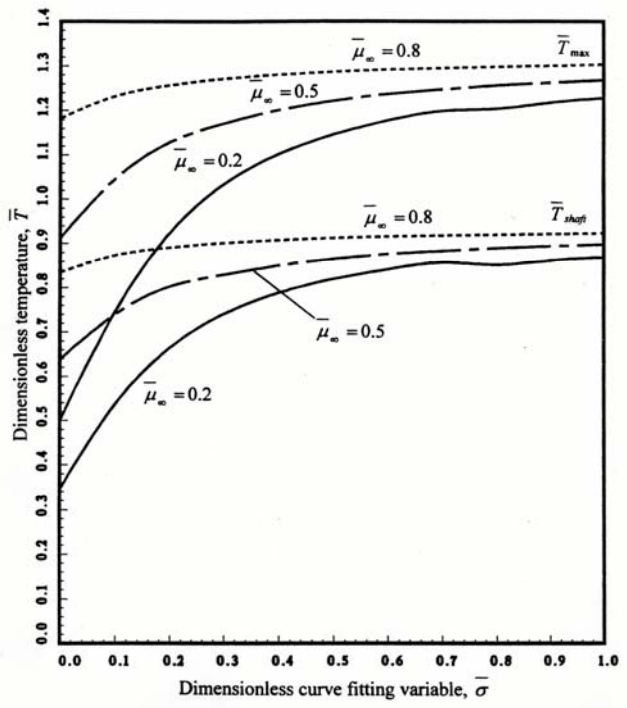

Figure 9 : Effect of curve fitting variable on the maximum temperature and shaft temperature of a journal bearing ($\varepsilon = 0.5$; $\Lambda = 1$; $\kappa_1 = 0.15$; $\kappa_2 = 1.5$)

Figure 9 shows how $\overline{T}_{max}$ and $\overline{T}_{shaft}$ vary with $\overline{\sigma}$. At a relatively low $\overline{\sigma}$, both $\overline{T}_{max}$ and $\overline{T}_{shaft}$ increase rapidly since the non-Newtonian viscosity is not stable. At a relatively large $\overline{\sigma}$, the variation of $\overline{T}_{max}$ and $\overline{T}_{shaft}$ tends to become very small since the non-Newtonian viscosity is more stable. The effect of non-Newtonian reduces as $\overline{\mu}_\infty$ increases and, therefore, the variation of $\overline{T}_{max}$ and $\overline{T}_{shaft}$ tends to become small.

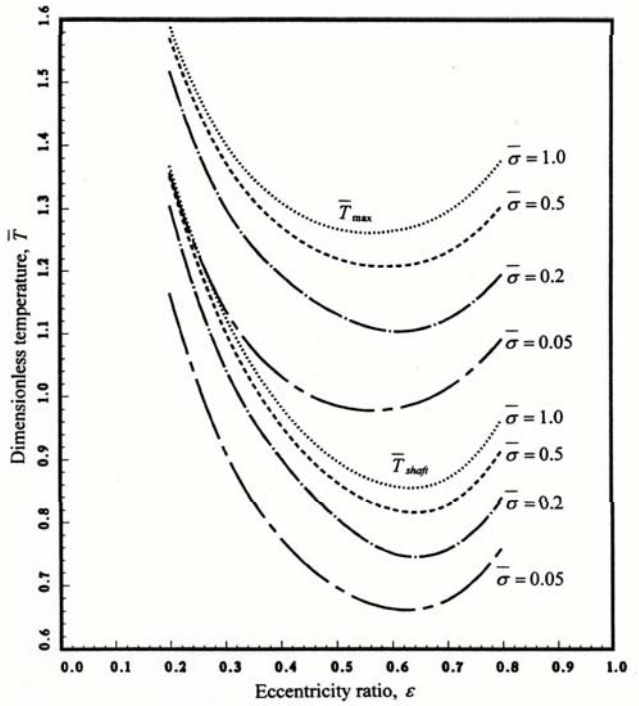

Figure 10 : Effect of eccentricity ratio on the maximum temperature and shaft temperature of a journal bearing. ($\overline{\mu}_\infty = 0.5$; $\Lambda = 1$; $\kappa_1 = 0.15$; $\kappa_2 = 1.5$)

Figure 10 shows how $\overline{T}_{max}$ and $\overline{T}_{shaft}$ vary with eccentricity ratio according to the ISOADI prediction. They are also computed at $\overline{\mu}_\infty$=0.5 and with the temperature rise parameters of κ_1=0.15 and κ_2=1.5. Figure 10 shows that at a fixed eccentricity ratio both $\overline{T}_{max}$ and $\overline{T}_{shaft}$ increase with increasing $\overline{\sigma}$ since the non-Newtonian viscosity remains stably high due to the high $\overline{\sigma}$. Similarly to Newtonian fluids, for the eccentricity ratio in the range $\varepsilon \leq 0.3$ or $\varepsilon \geq 0.7$ the maximum temperature $\overline{T}_{max}$ and the shaft temperature $\overline{T}_{shaft}$ tend to be large. At a low eccentricity ratio the leakage flow rate is very small and thus the bearing runs hot while the viscosity dissipation is small. At a high eccentricity ratio the leakage flow rate tends to cool the bearing but the viscous dissipation dominates.

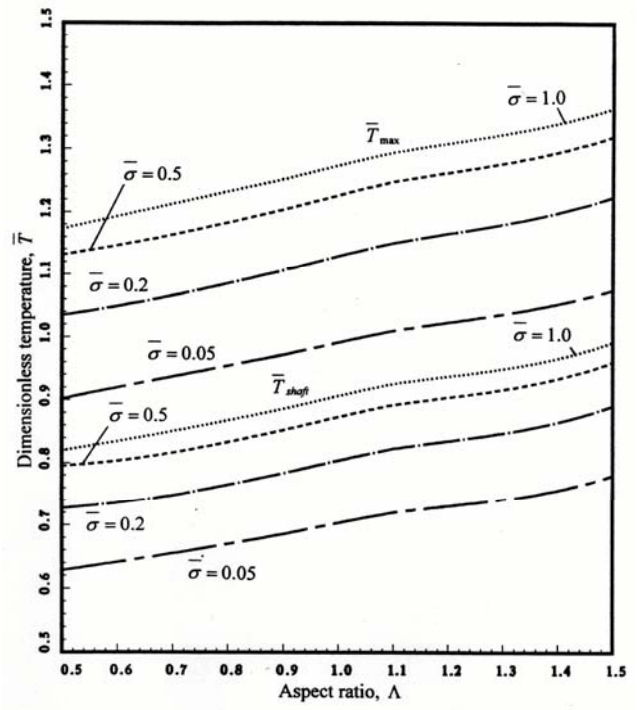

Figure 11 : Effect of aspect ratio on the maximum temperature and shaft temperature of a journal bearing. ($\overline{\mu}_\infty = 0.5$; $\varepsilon = 0.5$; $\kappa_1 = 0.15$; $\kappa_2 = 1.5$)

Figure 11 shows how $\overline{T}_{\max}$ and $\overline{T}_{\text{shaft}}$ vary with the aspect ratio $\Lambda = L/D$ according to the ISOADI predictions. Both $\overline{T}_{\max}$ and $\overline{T}_{\text{shaft}}$ tend to increase roughly linearly with increasing aspect ratio. Also, $\overline{T}_{\max}$ and $\overline{T}_{\text{shaft}}$ increase with increasing $\overline{\sigma}$.

4 Concluding Remarks

This paper is devoted to the analysis of thermal effect journal bearings lubricated with multigrade oils, which are known to exhibit shear-thinning behavior. The analysis incorporates two dimensionless temperature rise parameters κ_1 and $\kappa_2$in conjunction with dimensionless curve fitting variable $\overline{\sigma}$ and the dimensionless infinite-shear-rate viscosity $\overline{\mu}_\infty$to characterize the influence the temperature field for multigrade engine oils. Results of extensive amount of simulations attest to the importance of thermal effects in bearings. A series of charts are presented that can assist the designer to readily predict the maximum bearing temperature and the shaft temperature.

References

Buckholz, R. H. (1986): Effects of Power-Law, Non-Newtonian Lubricants on Load Capacity and Friction for Plane Slider Bearings, *Journal of Tribology*, vol. 108, pp. 86-91.

Dien, I. K. and Elrod, H. G. (1983): A Generalized Steady-State Reynolds Equation for Non-Newtonian Fluids with Application to Journal Bearing, *ASME Journal of Lubrication Technology*, vol. 105, pp. 385-390.

Dowson, D. (1962): A Generalized Reynolds Equation for Fluid Film Lubrication, *Int. J. Mech. Sc., Pergamon Press Ltd.*, vol. 4, pp. 159-170.

Dowson, D., Hudson, J. D., Hunter, B., and March, C. N. (1966-1967): An Experimental Investigation of the Thermal Equilibrium of Steadily Loaded Journal Bearings, *Proc. Instn. Mech. Engrs.*, v. 131, Part 3B, pp. 70-80.

Ferguson, J. and Kemblowski (1991): Applied Fluid Rheology, Elsevier Applied Science, London and New York.

Gecim, B. A. (1990): Non-Newtonian Effects of Multigrade Oils on Journal Bearing Performance, *Tribology Transactions*, vol. 33, pp. 384-394.

Khonsari, M. M. and Beaman, J. J. (1986): Thermohydrodynamic Analysis of Laminar Incompressible Journal Bearings, *ASLE Transactions*, pp. 141-150.

Khonsari, M. M. and Booser, E. R. (2001) *Applied Tribology – Bearing Design and Lubrication*, John Wiley & Sons, New York, NY.

Khonsari, M. M. Jang, J. Y. and Fillon, M. (1996): On the Generalization of Thermohydrodynamic Analyses for Journal Bearings, *Journal of Tribology*, vol. 118, pp. 571-579.

Paranjpe, R. S. (1992): Analysis of Non-Newtonian Effects in Dynamically Loaded Finite Journal Bearings Including Mass Conserving Cavitation, *Journal of Tribology*, v. 114, pp. 736-744.

Taner, R. I. (1963): Non-Newtonian Lubrication Theory and its Application to the Short Journal Bearing, *Austrian J. of Applied Science*, vol. 14, pp. 29-36.

Wada, S. and Hayashi, H. (1971): Hydrodynamic Lubrication of Journal Bearings by Pseudo-Plastic Lubricants (Part 1, Theoretical Studies), *Bulletin of the JSME*, vol. 14, pp. 268-278.

Wada, S. and Hayashi, H. (1971): Hydrodynamic Lubrication of Journal Bearings by Pseudo-Plastic Lubricants (Part 2, Experimental Studies), *Bulletin of the JSME*, vol. 14, pp. 279-286.

Wright, B., van Os, N. M., and Lyons, J. A. (1983): European Activity Concerning Engine Oil Classification-Part IV-The Effects of Shear Rate and Temperature on the Viscosity of Multigrade Oils, *SAE* Paper 830027.